

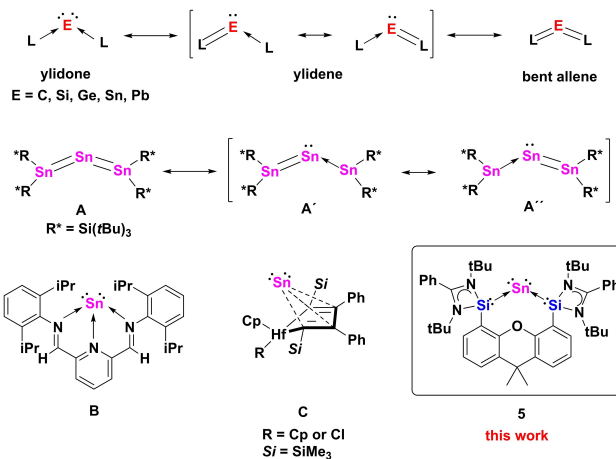


# A Genuine Stannyllone with a Monoatomic Two-Coordinate Tin(0) Atom Supported by a Bis(silylene) Ligand

Jian Xu, Chenshu Dai, Shenglai Yao, Jun Zhu, and Matthias Driess\*

**Abstract:** The monoatomic zero-valent tin complex (stannyllone)  $\{[Si^{II}(Xant)Si^{II}]Sn^0\}$  **5** stabilized by a bis(silylene)xanthene ligand,  $[Si^{II}(Xant)Si^{II} = PhC(NtBu)_2Si(Xant)Si(NtBu)_2CPh]$ , and its bis-tetracarbonyliron complex  $\{[Si^{II}(Xant)Si^{II}]Sn^0[Fe(CO)_4]_2\}$  **4** are reported. The stannyllone **5** bearing a two-coordinate zero-valent tin atom is synthesized by reduction of the precursor **4** with potassium graphite. Compound **4** results from the  $Sn^{II}$  halide precursor  $\{[Si^{II}(Xant)Si^{II}]Sn^0Cl\}Cl$  **2** or  $\{[Si^{II}(Xant)Si^{II}]SnBr_2\}$  **3** through reductive salt-metathesis reaction with  $K_2Fe(CO)_4$ . According to density functional theory (DFT) calculations, the highest occupied molecular orbital (HOMO) and HOMO-1 of **5** correspond to a  $\pi$ -type lone pair with delocalization into both adjacent vacant orbitals of the  $Si^{II}$  atoms and a  $\sigma$ -type lone pair at the  $Sn^0$  center, respectively, indicating genuine stannyllone character.

Monoatomic zero-valent metal complexes are very well established in transition-metal chemistry.<sup>[1]</sup> In contrast, related compounds of the main-group elements are far less explored. Efforts to realize isolable monoatomic zero-valent Group 14 underwent a boost when Frenking and co-workers reinterpreted the donor–acceptor interactions in carbodiphosphorane based on quantum chemical analysis, showing that the compound has a diphosphine carbon(0) complex character.<sup>[2]</sup> As a consequence, the existence of a new series of complexes with the general form  $L: \rightarrow E^0 \leftarrow :L$  ( $L = \sigma$ -donor,  $E = C, Si, Ge, Sn, Pb$ ; Scheme 1) was predicted theoretically.<sup>[3]</sup> In addition, the term “ylidone” ( $E = C$ : carbene;  $Si$ , silyllone;  $Ge$ , germyllone;  $Sn$ , stannyllone;  $Pb$ , plumblyllone) was given to this type of compounds.<sup>[3b]</sup> Owing to the zero-valent nature of the central atoms, which possess



**Scheme 1.** Top: General form of ylidenes, ylidones and bent-allene resonance structures. Mid: Tristannaallene **A** and its resonance structures **A'** and **A''**. Bottom: Examples of the  $Sn^0$  complexes **B**, **C**, and **5** of this work.

four valence electrons as two lone pairs, the synthesis of such isolable species has attracted much attention in the last decade. Utilizing different strong donor ligand systems, several isolable carbones, silyllones, and germyllones have been realized experimentally.<sup>[4–7]</sup> Moving down to the heaviest Group 14 elements, tin and lead, however, the synthesis of such complexes becomes rather difficult due to their intrinsic lability which readily leads to decomposition of the products as free ligands and elemental tin or lead. To date, a genuine two-coordinate stannyllone and plumblyllone featuring two lone pairs of electrons at the central  $Sn^0$  and  $Pb^0$  atom remain unknown.

By combining valence bond (VB) theory and maximum probability domain (MPD) approaches, Turek and co-workers suggested that heavy group 14 zero-valent complexes should be described as a resonating combination of ylidone and ylidene structures with a minor contribution of the bent allene form (Scheme 1).<sup>[8]</sup> Remarkably, the tristannaallene **A**<sup>[9]</sup> (Scheme 1), reported by Wiberg and co-workers in 1999, adopts a bent allene structure. According to the  $^{119}Sn$  NMR spectrum and theoretical calculations, **A** exhibits low-valent character with only one lone pair at the central tin atom. It was thus also described as a stannyllene adduct of a distannavinylidene (**A'** or **A''**). Employing a tridentate diiminopyridine, Flock and co-workers have obtained complex **B** (Scheme 1) containing a tin atom in the formal oxidation state of zero, which may also be described as a  $Sn^{II}$  complex due to the presence of a redox non-innocent

[\*] J. Xu, Dr. S. Yao, Prof. Dr. M. Driess  
 Department of Chemistry: Metalorganics and Inorganic Materials  
 Technische Universität Berlin,  
 Strasse des 17. Juni 115, Sekr. C2, 10623 Berlin (Germany)  
 E-mail: matthias.driess@tu-berlin.de

C. Dai, Prof. Dr. J. Zhu  
 State Key Laboratory of Physical Chemistry of Solid Surface and  
 Collaborative Innovation Center of Chemistry for Energy Materials  
 (iCHEM),  
 and College of Chemistry and Chemical Engineering,  
 Xiamen University, 361005 Xiamen (People's Republic of China)

© 2021 The Authors. Angewandte Chemie International Edition published by Wiley-VCH GmbH. This is an open access article under the terms of the Creative Commons Attribution License, which permits use, distribution and reproduction in any medium, provided the original work is properly cited.

ligand.<sup>[10]</sup> Notably, Saito and co-workers documented recently the  $\eta^4$ -butadiene  $\text{Sn}^0$  complex **C**<sup>[11]</sup> (Scheme 1) featuring some transition-metal-like behavior for a p-block metal. In recent years, we were interested in the chemistry of monoatomic zero-valent Group 14 complexes and succeeded in isolating several silylones and germylones with chelating bis(NHC) (NHC = *N*-heterocyclic carbene) and bis(NHSi) (NHSi = *N*-heterocyclic silylene) chelating ligands, respectively.<sup>[6c-e,7d-f]</sup> Herein, we report the synthesis of the genuine stannylone **5** with a monoatomic two-coordinate  $\text{Sn}^0$  atom supported by a bis(NHSi)xanthene ligand (Scheme 1) and its bis- $\text{Fe}(\text{CO})_4$  complex **4**. The structures of **2**, **3**, **4** and **5** were confirmed by X-ray crystallographic studies.<sup>[12]</sup>

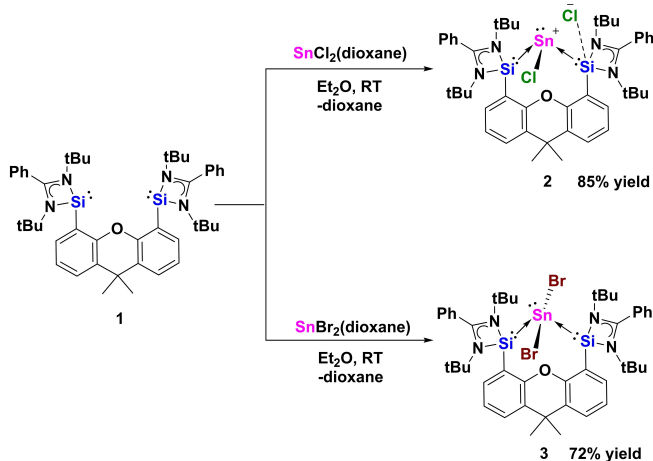
Starting from the chelating bis(NHSi)xanthene  $\text{Si}^{\text{II}}$ -(Xant) $\text{Si}^{\text{II}}$  ligand **1**,<sup>[13]</sup> the reaction with one molar equivalent of  $\text{SnCl}_2$ (dioxane) and  $\text{SnBr}_2$ (dioxane) in  $\text{Et}_2\text{O}$  at room temperature resulted in a yellow precipitate of the bis(NHSi)- $\text{Sn}^{\text{II}}$  halide complexes  $\{[\text{Si}^{\text{II}}(\text{Xant})\text{Si}^{\text{II}}]\text{SnCl}\}\text{Cl}$  **2** and  $\{[\text{Si}^{\text{II}}(\text{Xant})\text{Si}^{\text{II}}]\text{SnBr}_2\}$  **3**, which were isolated in 85 % and 72 % yields, respectively (Scheme 2). The  $^{29}\text{Si}$  NMR spectra of **2** and **3** show a singlet at  $\delta = 29.4$  ppm ( $^1J_{\text{Si, Sn}} = 1334$  Hz) and 30.3 ppm ( $^1J_{\text{Si, Sn}} = 1350$  Hz) with  $^{119}\text{Sn}$ -satellites, respectively, downfield-shifted with respect to that of **1** ( $\delta =$

17.3 ppm). The  $^{119}\text{Sn}$  NMR spectra show a singlet at  $\delta = -348.1$  ppm for **2** and  $\delta = -392.0$  ppm for **3**.

The molecular structure of **2** established by X-ray diffraction (XRD) reveals a bis(NHSi) supported  $\text{Sn}^{\text{II}}$  center bonded to a chlorine atom (Cl1) and a stereoactive lone pair, adopting a trigonal-pyramidal coordination geometry (Figure 1 left). The remaining chloride anion Cl2 shows a weak interaction with one of the silicon atoms (Si2...Cl2: 2.52(2) Å) akin to the situation in previously reported analogous chlorogermilymylidene chloride.<sup>[7e]</sup> In the case of **3** (Figure 1 middle), the central  $\text{Sn}^{\text{II}}$  atom is four-coordinate. Featuring also a stereoactive lone pair, the  $\text{Sn}^{\text{II}}$  center adopts a see-saw geometry with two bromine atoms (Br1-Sn1-Br2: 165.79(13)°).

Following the successful approach for the synthesis of silylones<sup>[6]</sup> and germylones,<sup>[7]</sup> we attempted to synthesize a stannylone through reduction of **2** and **3** with  $\text{KC}_8$  or  $\text{Na}(\text{C}_{10}\text{H}_8)$  but failed. Presumably, the thus-formed zero-valent tin complex supported by the strong  $\sigma$ -donating bis(NHSi) ligand is too sensitive under the harsh reducing conditions. Considering our previous success of synthesizing the bis(NHSi)pyridine germylone iron carbonyl complex  $\{[\text{SiNSi}]\text{Ge}^0 \rightarrow \text{Fe}(\text{CO})_4\}$ ,<sup>[14]</sup> the introduction of  $\text{Fe}(\text{CO})_4$  as a Lewis acid may increase the stability of the desired stannylone. Compound **2** was thus mixed with 1.2 molar equivalents of Collman's reagent,<sup>[15]</sup>  $[\text{K}_2\text{Fe}(\text{CO})_4]$ , in THF and stirred overnight at room temperature, leading to the desired bis- $\text{Fe}(\text{CO})_4$  stannylone complex **4** in 42 % yields (Scheme 3). The mechanism of **4** is still unknown, however, we reasoned that reduction of **2** and **3** with  $\text{K}_2\text{Fe}(\text{CO})_4$  firstly affords the 1:1  $\text{Fe}(\text{CO})_4$  complex **4'** similar to  $\{[\text{SiNSi}]\text{Ge}^0 \rightarrow \text{Fe}(\text{CO})_4\}$ <sup>[14]</sup> as an intermediate (Scheme 3). Compound **4'** could be labile with respect to liberation of "free"  $\text{Fe}(\text{CO})_4$  which, in turn, reacts with intact **4'** to afford the bis- $\text{Fe}(\text{CO})_4$  complex **4** as final product.

The  $^{29}\text{Si}$  NMR spectrum of **4** shows a singlet at  $\delta = 27.0$  ( $^1J_{\text{Si, Sn}} = 1312$  Hz) ppm, while the  $^{119}\text{Sn}$  NMR spectrum exhibits a singlet at  $\delta = 7.3$  ppm. The molecular structure of **4** displays a bis(NHSi)-supported central Sn atom coordinated to two independent  $\text{Fe}(\text{CO})_4$  moieties in a distorted tetrahedral geometry (Figure 1 right). The Sn-Si distances in **4** (2.68(11) and 2.70(12) Å) are comparable to those values in **2** and **3** (2.62–2.71 Å), respectively. The Sn-Fe distances of 2.60(7) Å and 2.65(9) Å are considerably longer



**Scheme 2.** Synthesis of the bis(NHSi)- $\text{Sn}^{\text{II}}$  halide complexes **2** and **3** from bis(NHSi) **1**.

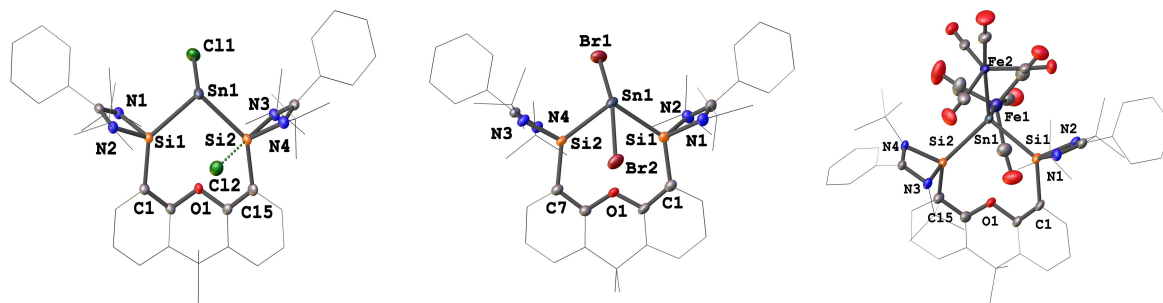
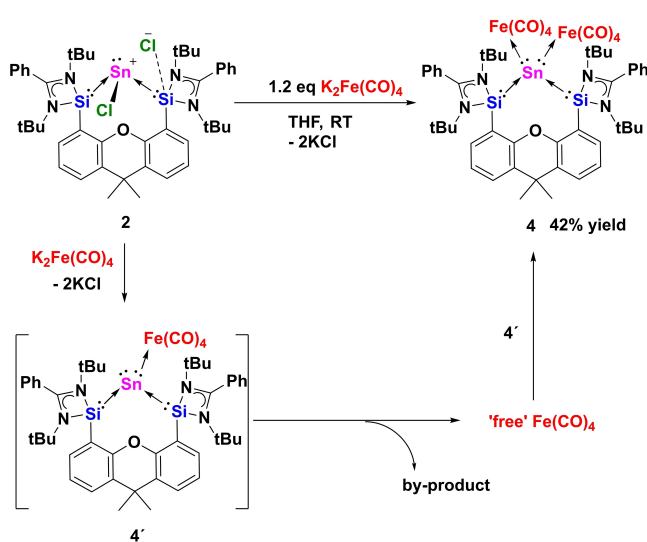


**Figure 1.** Molecular structures of **2**, **3** and **4**.<sup>[12]</sup> Thermal ellipsoids are drawn at the 50% probability level. H atoms and solvent molecules are omitted for clarity.



**Scheme 3.** Formation of diiron carbonyl stannylone complex **4** via **4'** from **2**.

than those observed in related  $\text{Sn}^{\text{II}} \rightarrow \text{Fe}(\text{CO})_4$  complexes (ca. 2.40–2.50 Å).<sup>[16]</sup> The IR stretching vibrations of CO in **4** appear at 1962, 1881 and 1834  $\text{cm}^{-1}$ , which are significantly red-shifted compared to the values of a carbonyl *N*-heterocyclic stannylene iron complex (2055, 1973, and 1953  $\text{cm}^{-1}$ ).<sup>[17]</sup> This indicates that the  $\text{Sn}^0$  center of **4** is a stronger electron donor than the stannylene- $\text{Sn}^{\text{II}}$  atoms, despite that the capability of the latter stannylene- $\text{Sn}^{\text{II}}$  atoms as  $\pi$ -acceptors should not be ignored.

To gain an insight into the electronic structure of **4**, we performed density functional theory (DFT) calculations with the Gaussian16 (Revision A.03) program.<sup>[18]</sup> All structures were optimized at the PEB0-D3BJ/Def2-SVP ~ ma-TZVP level of theory in the gas phase due to the smallest relative mean deviation (RD) of structural parameters in comparison with the metric data from X-ray structure analyses. No imaginary frequency was obtained at the same level, confirming a local minima. The full sets of calculated geometries and energies are given in Supporting Information.

The principal interacting orbital (PIO) analysis<sup>[19]</sup> evaluates the strength of orbital interactions via PIO-based bond index (PBI). As a result, we found four dominating  $\sigma$ -type interactions between the Sn and other bonded atoms (Figure 2). The second and third PIO pairs correspond to two dative bonds between Sn and two Si atoms with close-to-one PBI values, 0.91 and 0.88, respectively. Specifically, the Sn atom utilizes its 5*p* orbitals to form two Sn–Si bonds with contributions of 1.31 e/1.35 e from Si and 0.69 e/0.65 e from Sn. For the first PIO pair, the lone pair electrons on the *p*-orbital of Sn atom are decreased to 0.88 e, caused by  $\sigma$ -donation to *d*-orbitals of Fe. In other words, the Sn atom in **4** accepts electrons from the two adjacent donor  $\text{Si}^{\text{II}}$  atoms and donates electrons to Fe, forming four dative bonds with the Si and Fe atoms. Furthermore, these four donating interactions between Sn and four adjacent atoms (two Si and two Fe) are consistent with the results of the natural adaptive orbital (NAO) analysis<sup>[20]</sup> (Figure S28). Specifi-

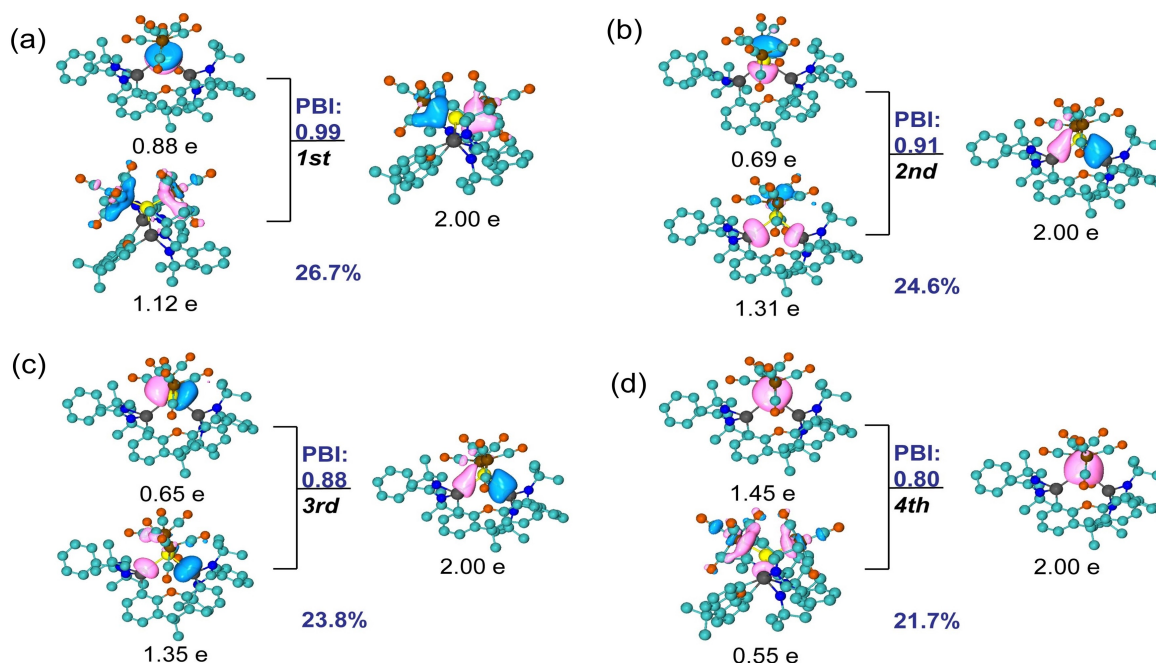
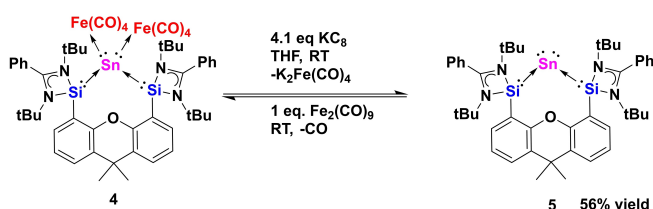


**Figure 2.** PIO analysis on the bonding modes of Sn–Si and Sn–Fe<sub>4</sub> in compound **4**. The compound **4** is decomposed to two moieties, the Sn atom and the rest. Hydrogen atoms in 3D structures are omitted for clarity. The total PBI value of two fragments is 3.68. The isosurface 0.050 au is plotted.

cally, four  $\sigma$ -type NAdOs are determined with close-to-one eigenvalues, 0.826, 0.806, 0.703 and 0.660, respectively.

Since compound **4** can be considered as a carbonyl stannylone iron complex with a tin center in the formal zero oxidation state, it could be a more suitable precursor to generate the desired stannylone than **2** and **3**. In order to eliminate the  $[\text{Fe}(\text{CO})_4]$  moieties as  $[\text{Fe}(\text{CO})_4]^{2-}$  leaving groups, **4** was allowed to react with  $\text{KC}_8$  in a molar ratio of 1:4.1 in THF and stirred at room temperature for six hours (Scheme 4). To our delight, the desired reductive elimination of  $[\text{Fe}(\text{CO})_4]$  succeeds and leads to the formation of the dark blue stannylone **5** which could be isolated in 56% yields from the reaction mixture. The dark blue color of **5** fades immediately when exposed to air, indicating its high sensibility towards oxygen and moisture. In the solid state, stannylone **5** can be stored under  $\text{N}_2$  atmosphere. However, it does gradually decompose into elemental tin and free bis(NHSi)xanthene ligand **1** in solutions (NMR). The  $^{29}\text{Si}$  NMR spectrum of **5** shows a singlet at  $\delta=50.6$  ppm with  $^{119}\text{Sn}$ -satellites ( $^1J_{\text{Si,Sn}}=1244$  Hz), downfield-shifted relative to **4** ( $\delta=27.0$  ppm) and **1** ( $\delta=17.3$  ppm). The  $^{119}\text{Sn}$  NMR spectrum exhibits a singlet at  $\delta=-1147.2$  ppm, dramatically highfield-shifted with respect to that of **4** ( $\delta=7.3$  ppm). The enormous upfield shift observed for **5** is confirmed by Gauge-Independent Atomic Orbital (GIAO) calculations ( $\delta_{\text{cal.}}=-1325.5$  ppm, Supporting Information). We reasoned that the remarkable shielding of the  $^{119}\text{Sn}$  nucleus in **5** is caused by the two “free” lone-pairs of electrons at the  $\text{Sn}^0$  center. In addition, **5** can be converted back to **4** by reaction with  $\text{Fe}_2(\text{CO})_9$  in THF under release of CO (Scheme 4).

Compound **5** crystallizes in the monoclinic space group  $P2_1/c$  with two independent molecules in the asymmetric unit (Figure 3). The central  $\text{Sn}^0$  atoms are coordinated by



**Scheme 4.** Conversion of complex **4** to stannylone **5** with  $\text{KC}_8$  and its reversed reaction with  $\text{Fe}_2(\text{CO})_9$ .

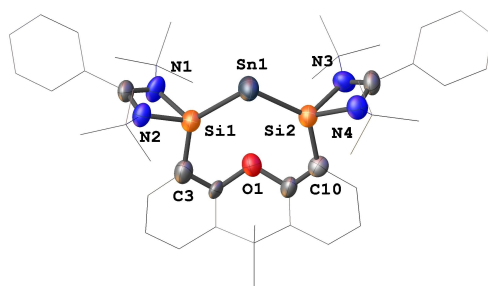
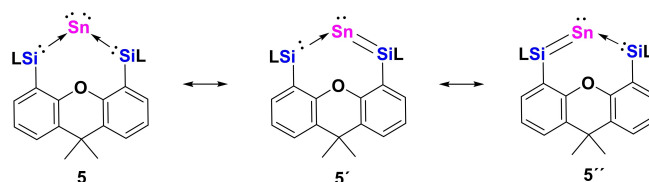


**Figure 3.** Molecular structure of **5**.<sup>[22]</sup> The asymmetric unit contains two independent molecules, only one is depicted. Thermal ellipsoids are drawn at the 50% probability level. H atoms are omitted for clarity.

the two  $\text{Si}^{\text{II}}$  atoms of the bis(NHSi) donor with the  $\text{Si1-Sn1-Si2}$  angles of  $99.34(10)^\circ$  and  $100.10(9)^\circ$ , respectively. The  $\text{Si-Sn}$  distances, ranging from  $2.51(3)$  to  $2.54(3)$  Å, are significantly shorter than those in **4** ( $2.68(11)$  and  $2.70(12)$  Å) and intermediate between a  $\text{Sn-Si}$  double [ $(2.42(14)$  Å)]<sup>[21]</sup> and  $\text{Si-Sn}$  single bond lengths of  $2.60$  Å.<sup>[22]</sup>

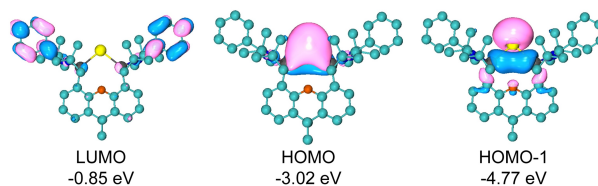
Also, we performed a PIO analysis for **5** and found two  $\sigma$ -types and a  $\pi$ -type interaction between the Sn and two Si atoms (Figure 4b). The first and third PIO pairs correspond to  $\sigma$ -type dative interaction with close-to-one PBI values, 0.92 and 0.81, respectively, similar to those of **4**. In addition, the  $\pi$ -type delocalization between Sn and the two Si atoms could be formed by the lone pair electrons of a  $5p$  orbital on the Sn atom interacting with the adjacent vacant  $3p$  orbitals of the Si atoms. The larger fuzzy bond order than 1.0 (approximately 1.3) for  $\text{Sn-Si}$  is also the result of a  $\pi$ -type delocalization. Furthermore, these three primary interactions between Sn and the two Si atoms are supported by NAdO analysis (Figure S30), where two  $\sigma$ -type and a  $\pi$ -type NAdOs were located with close-to-one Eigenvalues, 0.866, 0.825 and 0.661, respectively. As shown in Figure 4a, the HOMO-1 and HOMO, respectively, correspond to a  $\sigma$ -lone pair and a  $\pi$ -lone pair on the  $\text{Sn}^0$  atom. The latter is significantly delocalized into the adjacent Si atoms. In addition to the ylidone structure of **5**, we thus propose the relevance of the two ylidene resonance structures **5'** and **5''** (Scheme 5). The UV/Vis spectrum of **5** recorded in toluene displays an intense absorption at 674 nm with the absorptivity  $\epsilon_{\text{max}}/(\text{M}^{-1}\text{cm}^{-1})$  of 3088 (Figure S22). According to time-dependent DFT (TD-DFT) calculations,<sup>[23]</sup> the observed peak ( $\lambda_{\text{ex}}=674$  nm,  $\lambda_{\text{TD-DFT}}=672$  nm) is mainly assigned to the  $\text{S}_1$  state (Table S14), which corresponds to the  $\pi$ - $\pi^*$  excitation from HOMO to LUMO. Notably, the band is more red-shifted than that of the silicon (silylone, 569 nm)<sup>[6d]</sup> and germanium (germylone, 596 nm)<sup>[7a]</sup> homologues.

In summary, while the common reductive approach to access a monoatomic zero-valent Group 14 compounds failed in the case of the the  $\text{Sn}^{\text{II}}$  halide precursors  $\{[\text{Si}^{\text{II}}(\text{Xant})\text{Si}^{\text{II}}]\text{Sn}^{\text{II}}\text{Cl}\}\text{Cl}$  **2** and  $\{[\text{Si}^{\text{II}}(\text{Xant})\text{Si}^{\text{II}}]\text{Sn}^{\text{II}}\text{Br}_2\}$  **3**, we could accomplish an iron-mediated reduction of  $\text{Sn}^{\text{II}}$  in **2** and **3** to  $\text{Sn}^0$  in the stannylone-iron complex  $\{[\text{Si}^{\text{II}}(\text{Xant})\text{Si}^{\text{II}}]\text{Sn}^0[\text{Fe}(\text{CO})_4]_2\}$  **4** using  $\text{K}_2\text{Fe}(\text{CO})_4$ . Reductive elimination of the  $[\text{Fe}(\text{CO})_4]$  groups of **4**, in turn, with  $\text{KC}_8$  enabled the synthesis and isolation of the first bis(silylene)-stabilized stannylone **5**. Its electronic structure and presence of a genuine two-coordinate  $\text{Sn}^0$  center have been elucidated by DFT calculations. The HOMO and HOMO-1 of **5** correspond to a  $\pi$ -type lone pair, with delocalization into both



**Scheme 5.** Proposed resonance structures of stannylone **5** [ $\text{L}=\text{PhC}(\text{N}t\text{Bu})_2$ ].

## (a) Molecular orbitals



## (b) PIO analysis

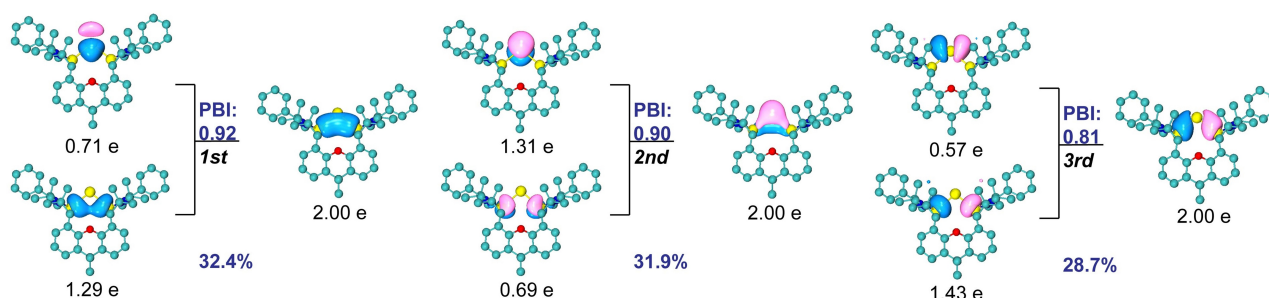


**Figure 4.** a) Molecular orbitals. b) PIO analysis on the bonding modes of Sn–Si in compound **5**. The compound **5** is decomposed to two moieties, the Sn atom and the rest. Hydrogen atoms in 3D structures are omitted for clarity. The total PBI value of two fragments is 2.83. The isosurface 0.050 au is plotted.

adjacent Si<sup>III</sup> vacant orbitals, and a  $\sigma$ -type lone pair at the Sn<sup>0</sup> center, respectively, indicating a genuine stannylone character. Further investigations on the reactivity of **5** are currently in progress.

## Acknowledgements

This work was funded by DFG (German Research Foundation) under Germany's Excellence Strategy—EXC 2008-390540038—UniSysCat and DR-226/21-1. We are grateful for financial support by the China Scholarship Council. Open Access funding enabled and organized by Projekt DEAL.

## Conflict of Interest

The authors declare no conflict of interest.

**Keywords:** Carbonyl Iron Complexes · Chelate ligands · Stannylone · Silylene · Tin

- [1] J. F. Hartwig, *Organotransition metal chemistry: from bonding to catalysis*, University Science Books, Mill Valley, **2010**.  
 [2] R. Tonner, F. Öxler, B. Neumüller, W. Petz, G. Frenking, *Angew. Chem. Int. Ed.* **2006**, *45*, 8038–8042; *Angew. Chem.* **2006**, *118*, 8206–8211.  
 [3] a) G. Frenking, R. Tonner, *Pure Appl. Chem.* **2009**, *81*, 597–614; b) N. Takagi, T. Shimizu, G. Frenking, *Chem. Eur. J.* **2009**,

- 15*, 8593–8604; c) G. Frenking, R. Tonner, S. Klein, N. Takagi, T. Shimizu, A. Krapp, K. K. Pandey, P. Parameswaran, *Chem. Soc. Rev.* **2014**, *43*, 5106–5139.  
 [4] a) S. Yao, Y. Xiong, M. Driess, *Acc. Chem. Res.* **2017**, *50*, 2026–2037; b) P. K. Majhi, T. Sasamori, *Chem. Eur. J.* **2018**, *24*, 9441–9455; c) M. Driess, S. Yao, Y. Xiong, A. M. Saddington, *Chem. Commun.* **2021**, *57*, 10139–10153.  
 [5] C. A. Dyker, V. Lavallo, B. Donnadieu, G. Bertrand, *Angew. Chem. Int. Ed.* **2008**, *47*, 3206–3209; *Angew. Chem.* **2008**, *120*, 3250–3253.  
 [6] a) S. Ishida, T. Iwamoto, C. Kabuto, M. Kira, *Nature* **2003**, *421*, 725–727; b) K. C. Mondal, H. W. Roesky, M. C. Schwarzer, G. Frenking, B. Niepötter, H. Wolf, R. Herbst-Irmer, D. Stalke, *Angew. Chem. Int. Ed.* **2013**, *52*, 2963–2967; *Angew. Chem.* **2013**, *125*, 3036–3040; c) Y. Xiong, S. Yao, S. Inoue, J. D. Epping, M. Driess, *Angew. Chem. Int. Ed.* **2013**, *52*, 7147–7150; *Angew. Chem.* **2013**, *125*, 7287–7291; d) Y. Wang, M. Karni, S. Yao, A. Kaushansky, Y. Apeloig, M. Driess, *J. Am. Chem. Soc.* **2019**, *141*, 12916–12927; e) S. Yao, A. Kostenko, Y. Xiong, A. Ruzicka, M. Driess, *J. Am. Chem. Soc.* **2020**, *142*, 12608–12612.  
 [7] a) T. Iwamoto, T. Abe, C. Kabuto, M. Kira, *Chem. Commun.* **2005**, 5190–5192; b) T. Iwamoto, H. Masuda, C. Kabuto, M. Kira, *Organometallics* **2005**, *24*, 197–199; c) Y. Li, K. C. Mondal, H. W. Roesky, H. Zhu, P. Stollberg, R. Herbst-Irmer, D. Stalke, D. M. Andrada, *J. Am. Chem. Soc.* **2013**, *135*, 12422–12428; d) Y. Xiong, S. Yao, G. Tan, S. Inoue, M. Driess, *J. Am. Chem. Soc.* **2013**, *135*, 5004–5007; e) Y. Wang, M. Karni, S. Yao, Y. Apeloig, M. Driess, *J. Am. Chem. Soc.* **2019**, *141*, 1655–1664; f) S. Yao, A. Kostenko, Y. Xiong, C. Lorent, A. Ruzicka, M. Driess, *Angew. Chem. Int. Ed.* **2021**, *60*, 14864–14868; *Angew. Chem.* **2021**, *133*, 14990–14994.  
 [8] J. Turek, B. Braïda, F. De Proft, *Chem. Eur. J.* **2017**, *23*, 14604–14613.  
 [9] N. Wiberg, H. W. Lerner, S. K. Vasisht, S. Wagner, K. Karaghiosoff, H. Nöth, W. Ponikwar, *Eur. J. Inorg. Chem.* **1999**, 1211–1218.

- [10] J. Flock, A. Suljanovic, A. Torvisco, W. Schoefberger, B. Gerke, R. Pöttgen, R. C. Fischer, M. Flock, *Chem. Eur. J.* **2013**, *19*, 15504–15517.
- [11] T. Kuwabara, M. Nakada, J. Hamada, J. D. Guo, S. Nagase, M. Saito, *J. Am. Chem. Soc.* **2016**, *138*, 11378–11382.
- [12] Deposition Numbers 2110196 (for **2**), 2110197 (for **3**), 2110198 (for **4**), and 2110199 (for **5**) contain the supplementary crystallographic data for this paper. These data are provided free of charge by the joint Cambridge Crystallographic Data Centre and Fachinformationszentrum Karlsruhe Access Structures service [www.ccdc.cam.ac.uk/structures](http://www.ccdc.cam.ac.uk/structures).
- [13] Y. Wang, A. Kostenko, S. Yao, M. Driess, *J. Am. Chem. Soc.* **2017**, *139*, 13499–13506.
- [14] Y.-P. Zhou, M. Karni, S. Yao, Y. Apeloig, M. Driess, *Angew. Chem. Int. Ed.* **2016**, *55*, 15096–15099; *Angew. Chem.* **2016**, *128*, 15320–15323.
- [15] G. L. Miessler, D. A. Tarr, *Inorganic chemistry*, Pearson, Upper Saddle River, **2004**.
- [16] V. N. Khrustalev, I. A. Portnyagin, M. S. Nechaev, S. S. Bukalov, L. A. Leites, *Dalton Trans.* **2007**, 3489–3492.
- [17] A. Jana, R. Azhakar, H. W. Roesky, I. Objartel, D. Stalke, *Z. Anorg. Allg. Chem.* **2011**, *637*, 1795–1799.
- [18] M. Frisch, G. Trucks, H. Schlegel, G. Scuseria, M. Robb, J. Cheeseman, G. Scalmani, V. Barone, G. Petersson, H. Nakatsuji, Gaussian, Inc. Wallingford, CT, **2016**.
- [19] a) J. X. Zhang, F. K. Sheong, Z. Lin, *Chem. Eur. J.* **2018**, *24*, 9639–9650; b) J. X. Zhang, F. K. Sheong, Z. Lin, *WIREs Comput. Mol. Sci.* **2020**, *10*, e1469.
- [20] J. L. Casals-Sainz, A. Fernández-Alarcón, E. Francisco, A. Costales, A. Martín Pendas, *J. Phys. Chem. A* **2020**, *124*, 339–352.
- [21] A. Sekiguchi, R. Izumi, V. Y. Lee, M. Ichinohe, *J. Am. Chem. Soc.* **2002**, *124*, 14822–14823.
- [22] M. G. Voronkov, A. N. Egorochkin, *The Chemistry of Organic Germanium, Tin and Lead Compounds*, Wiley, New York, **1995**, chap. 2.
- [23] A. V. Marenich, C. J. Cramer, D. G. Truhlar, *J. Phys. Chem. B* **2009**, *113*, 6378–6396.

Manuscript received: October 17, 2021

Accepted manuscript online: November 17, 2021

Version of record online: December 1, 2021